New Time-Frequency Analysis of Acoustic Data

Yih-Nen Jeng*, Jia-Ming Huang[2] and Jia-Lin Tsai[2]
Department of Aeronautics and Astronautics
National Cheng-kung University
Tainan, Taiwan
*z6208016@email.ncku.edu.tw

You-Chi Cheng[3]
Department of Electric Engineering
National Taiwan University

ABSTRACT

A new time-frequency transform is employed to examine acoustic data of an old motorcycle, an Unmanned Aerial Vehicle (UAV), and an F-16 fighter. For a given data string, zero points around the two ends are identified by searching and interpolation. After dropping segments beyond two zero ends, the corresponding Fourier sine spectrum is obtained. The time-frequency transform imposes finite bandwidth window upon the Fourier sine spectrum centered at a given frequency. The inverse Fourier transform of the band-pass limited spectrum gives the real part of the resulting spectrogram. This procedure avoids the error induced by the finite data length and excessive average other than the Fourier transform. By carefully inspecting the real part plots of the spectrogram, one can pick many information about the structure vibration and aero-acoustic data. For the motorcycle data, a series of structure vibration modes and random vibration from low to high frequency oscillations are grasped. The minor frequency shifts of high frequency modes with respect to time and random vibration show that the motorcycle is not at a good condition. The UAV is a helicopter and the examined data covers the fuel run out of point. Around the low frequency regime, the wind produces ultrasonic acoustic signal and is captured by the spectrogram. After the fuel run out of instant, propellers do not gain power to rotate again and gradually lost the rotation speed so that all the corresponding modes show a linearly decayed frequency. The spectrogram of F-16 noise recorded in the cockpit reflects the harmonic and sub-harmonic modes of engine rotor and aero-acoustic of jet plume which may or may not interact with the wing-body and canopy structure. In the high frequency regime, the random noise modes may be emitted by interaction between aero-acoustic and structure at the transonic fly. These test cases show that sound records do carry valuable information and can be uncovered by the spectrogram generated by the new time-frequency transform.

Keywords: new time-frequency transform, Fourier sine spectrum, acoustic data, wave modes.

INTRODUCTION

Because of the rapid development of computer hard and software, the number and size of collected data strings show exponentially growth. As a consequence, to collect complicated data in outdoor environment and analyze them become more and more important. Among many available information, the acoustic signal is relatively easy to be collected. In addition, there are many information transferred through the solid, liquid, and gas in terms of pressure wave. Specifically, a acoustic signal may involve information related to speech, structure vibration, fluid motion, and wave propagation etc.. Since the propagation ranges of many sound sources are generally long enough, an acoustic signal may be too complicated to be analyzed.

To study such a complicated data string, the Fourier spectrum is not enough because it uses fixed Fourier coefficients (spectrum) over the expansion range. For time series data, as noted by Farge [1], a time frequency analyzing tool can capture the variation of spectrum with respect to time which reflects the involved details and mechanism(s). Therefore, spectrograms generated by time frequency transforms, such as short time Fourier, Gabor and wavelet transforms, are widely applied [2,3]. Unfortunately, these methods can not reflect many detailed information of a complicated data sting.

Recently, the Fourier spectrum was re-studied in Ref. [4-5]. It is found that, most Fourier spectrums involve error introduced by the fact that all the necessary period conditions of a discrete data string can not be satisfied. The error will fade almost all the minor modes and slightly distort dominant modes. If the non- sinusoidal and discontinuous parts can be removed, and the Fourier sine spectrum is employed, the resulting spectrum will contain small error such that most information of an acoustic signal can be reflected correctly. Moreover, in Ref.[6-11], new time-frequency transforms basing on the Fourier sine spectrum were developed. In Ref.[10,11], a

[1] Professor, [2] Graduate Students, and [3]Bachelor.

new spectrogram generator was proposed, whose results has a much clearer visibility than that generated by all the existing transforms. The arrangement of Fourier sine spectrum and new spectrogram makes the precise data analysis of time series data possible. Therefore, it seems that it is the time to start the study about acoustic data collected from a complicated environment. Note that the wave components emitted from different sources may have different phases. The cancellation and/or enhancement between wave modes with nearby frequencies is an expected difficulty of wave decomposition. Nevertheless, because of the big economic reward, it is a worth effort to study this subject.

THEORETICAL ANALYSIS

The related works concerning to this study are the method of generating a Fourier sine spectrum, iterative filter with diffusive property, continuous wavelet transform, and modified Hilbert transform. For the sake of completely, they are briefly reviewed below.

1. Iterative Filter Using Gaussian Smoothing [12]

Assume that a discrete data string can be approximated by

$$y(t) = \sum_{n=0}^{N} b_n \cos\left(\frac{2\pi t}{\lambda_n}\right) + c_n \sin\left(\frac{2\pi t}{\lambda_n}\right) \qquad (1)$$

In Ref.[14, 23-25], it was proven that after applying the Gaussian smoothing method once, the resulting smoothed data becomes

$$\bar{y}_1(t) \approx \sum_{n=0}^{N} a(\sigma/\lambda_n)\{b_n \cos\left(\frac{2\pi t}{\lambda_n}\right) + c_n \sin\left(\frac{2\pi t}{\lambda_n}\right)\} \qquad (2)$$

$$0 \le a(\sigma/\lambda_n) \approx \exp[-2\pi^2\sigma^2/\lambda_n^2] \le 1$$

If the high frequency part is repeatedly smoothed m times by the Gaussian smoothing method, the corresponding results can be rearranged in the followings.

$$y_m' = \sum_{n=0}^{N} [1-a(\sigma/\lambda_n)]^m \left[b_n \cos\left(\frac{2\pi t}{\lambda_n}\right) + c_n \sin\left(\frac{2\pi t}{\lambda_n}\right)\right],$$

$$\bar{y}(m) = \bar{y}_1 + \bar{y}_2 + \ldots + \bar{y}_m = y - y_m'$$

$$= \sum_{n=0}^{N} A_{n,m,\sigma}\left[b_n \cos(2\pi t/\lambda_n) + c_n \sin(2\pi t/\lambda_n)\right] \qquad (3)$$

where y_i' and $\bar{y}_i$ are the high frequency and smoothed parts at i -th smoothing step. Finally, $\bar{y}(m)$ is the desired smooth part and y_m' is the high frequency part. Obviously, both the original Gaussian smoothing and iterative smoothing algorithms are diffusive. Suppose that all the waveforms within the range of $\lambda_{c1} < \lambda < \lambda_{c2}$ are insignificantly small. The above mentioned iterative smoothing procedure can be used as an effective filter to give both the low and high frequency parts without introducing any dispersive error.

2. Fourier Sine Spectrum with Small Error [4,5]

In general, if a Fast Fourier Transform algorithm (FFT) is employed to evaluate the spectrum of a data string with non-sinusoidal part, the resulting spectrum always has an exponentially decayed envelope. Similarly, the non-periodic condition often introduces a negative contribution. In Ref.[6-11], the above iterative filter is employed to remove the non-sinusoidal part and reduce the low frequency error. The complete procedures are as follows.

1. For the remaining high frequency part, use search and interpolation methods to find 0 points at two ends.
2. Use the following monotonic cubic interpolation [4,5,13] to redistribute the data and let the total number of points is set to be 2^m.
3. Perform an odd function mapping with respect to one end so that the final data point is doubled.
4. A simple FFT algorithm is employed to generate the desired Fourier sine spectrum.

The odd function mapping makes sure that the periodicity is valid up to the highest order of derivative the data can resolve. Consequently, the spectrum error can be effectively reduced.

3. Morlet Transform and Enhanced Version

For the data string of Eq.(1), the Morlet transform evaluates the wavelet coefficient by the formula [1-3].

$$W(a,\tau) = \frac{1}{\sqrt{a}} \int_{-\infty}^{\infty} y(t) e^{-i6(t-\tau)/a} e^{-(t-\tau)^2/(2a^2)} dt \qquad (4)$$

where a is called the scale function of the transform. Basically, it transform a one-dimensional data string into the plane (a,τ) where a is related to the wavelength or frequency and τ represents time scale. On the wavelet coefficient plane, one can extract limited detailed information because the visibility of the plat is not good enough [6,7]. If the original data is expressed in form of Eq.(1), the resulting wavelet coefficient is approximated by the following formulas.

$$\overline{W}(a,\tau,y) \approx \sqrt{\frac{\pi a}{2}} \left\{ \sum_{n=0}^{\infty} b_n \exp\left(-\frac{a^2}{2}\left[\frac{2\pi}{\lambda_n} - \frac{6}{a}\right]^2 \right) \exp\left[\frac{i2\pi\tau}{\lambda_n}\right] \right.$$

$$\left. + \sum_{n=0}^{\infty} c_n \exp\left(-\frac{a^2}{2}\left[\frac{2\pi}{\lambda_n} - \frac{6}{a}\right]^2 \right) \exp\left[-\frac{i2\pi\tau}{\lambda_n}\right] \right\} \qquad (5)$$

Obviously, for a give scale function a, an inspection upon this equation reveals that the maximum response

occurs at $\lambda \approx a\pi/3$. In some sense, Eq.(5) shows that result of the Morlet transform is a generalized band-passed spectrum.

One may argue that the Fourier spectrum is an averaged data over the expansion domain so that it is impossible to extract any time frequency information from spectrum. However, the explicit form of Eq.(7) reflects the key such that a time dependent spectrum can be obtained by imposing band-passed window upon the spectrum. In Ref.[6,8,9], an enhanced version was proposed. The version imposes a band-pass limited window on the Fourier sine spectrum and obtained a band-pass filtered data string to replace $y(t)$ of Eq.(4). Although the visibility of the spectrogram is improved, some undesired contaminations still exist here and there.

4. The Gabor Transform [2,3] and Enhancement

The following short time Fourier (or Gabor) transform maps the data $y(t)$ into the continuous Gabor coefficient [2,3].

$$G(f,\tau,k)=\frac{1}{\sqrt{a}}\int_{-\infty}^{\infty} y(t)\psi^{*}(f,t-\tau)dt$$
$$\psi(f,t-\tau)=\exp[i2\pi f(t-\tau)]\exp[-(t-\tau)^2/(2k^2)] \quad (6)$$

Due to the similar reason, the Gabor transform may involve too many information for a given frequency. In Ref.[7], the Gabor transform was enhanced by imposing band-pass limited window on spectrum to produce a modified $y(t)$ and get similar improvement as that of Ref.[6,8,9]. In Ref.[7], several examples show that the enhanced Morlet and Gabor transforms produce rather similar results.

5. Hilbert Transform and Modification [14]

For a data string $x(t)$, defined in the range of $-\infty < t < \infty$, the following Hilbert transform is the corresponding imaginary part provided that $x(t)$ does not involve any non-sinusoidal part [2,3].

$$\tilde{x}(t)=\int_{-\infty}^{\infty}\frac{x(\tau)}{\pi(t-\tau)}d\tau \quad (7)$$

Then the amplitude and frequency can be evaluated directly as follows.

$$z(t)=x(t)+i\tilde{x}(t)=A(t)e^{i\theta(t)}$$
$$A(t)=[x^2(t)+\tilde{x}^2(t)]^{1/2} \quad (8)$$
$$\theta(t)=\tan^{-1}[\frac{\tilde{x}(t)}{x(t)}]=2\pi f_o t$$

It was proven in Ref.[14] that, for a data string with a finite range, the Hilbert transform evaluated on the time domain has significantly large error around the two ends of the data string. Moreover, the error deeply penetrates into the interior region. To reduce the penetration effect, the original Hilbert transform is embedded by Gaussian kernel in the form of [14]

$$J[x(t)]=\int_{t_1}^{t_2}\frac{\exp[-(t-\tau)^2/(2\sigma^2)]x(t)}{\pi(t-\tau)\cdot erf(\sqrt{2}\pi f\sigma)}d\tau \quad (9)$$

For a data string of infinite domain, where $t_1 \to -\infty$ and $t_2 \to \infty$, $J[x(t)]$ is approximately equal to the Hilbert transform $\tilde{x}(t)$ with an infinitesimal error whenever $\sqrt{2\pi}\,f\sigma$ >4. Numerical experiments show that, if the following conditions subject to σ are satisfied, $J[x(t)]$ is almost equal to $\tilde{x}(t)$ and the error penetration distance of the former is much shorter than that of the latter.

$$\sigma > \lambda_{\min},\ \ \sigma > 4\lambda_{\max}/\sqrt{2\pi} \quad (10),$$

where $\lambda_{\min}$ and $\lambda_{\max}$ are the shortest and longest wavelength of the sinusoidal function $x(t)$. Whenever the first criterion is violated, for a discrete data string with finite t_1 and t_2, an oscillatory frequency distribution is found around locations where the local wavelength $\approx \lambda_{\min}$. The reason is that the convolution integration should accumulate enough information (from those points where the magnitude of Gaussian kernel function is of order one) to reflect the exact information. In Ref.[14], it is also shown that the error penetration distance of $J[x(t)]$ becomes shorter for a smaller σ. Since the original and modified Hilbert transforms are valid only for a sinusoidal data string, it is easy to extrapolate the data beyond the two ends. Consequently, the error becomes insignificant in the desired data range as will be shown later [14].

6. Proposed Time-Frequency Transformation

A careful inspection upon sections 3 and 4 reveals that the enhanced Morlet and Gabor transforms employ two successive transformations. Their second transformations introduce boundary error and excessive average due to integration. It is intuitive to employ the Fourier spectrum together with the band-passed windowing procedure as the only transformation. Therefore, for a data string without the discontinuous part, the following procedure of producing a new time frequency transformation is proposed:

1. Use the iterative filter of subsection 1 to remove the non-sinusoidal part.
2. Use Fourier transform of subsection 2 to generate spectrum with small error.
3. For a given frequency, choose a suitable bandwidth and find the corresponding spectrum of finite band-width by imposing band-passed filter to the spectrum. The band-pass filtered data is generated by the inverse Fourier transform.

4. The band-pass filtered data string is just the real part of new transformation corresponding to the specific frequency.
5. Use the Hilbert transform to find the corresponding imaginary part and hence amplitude and frequency.

If any mode centered at a specific frequency is desired, the band-pass filtered data string is the answer. In other words, the present transformation automatically involves the corresponding inverse transform.

RESULTS AND DISCUSSIONS

In Ref.[11], a vocalization of "hello" was examined by the original Gabor, enhanced Gabor, and the new transforms whose two-(left) and three-dimensional (right) amplitude plots are shown in Fig.1a, 1b, and 1c, respectively. Obviously, the main features are captured in the three figures. However, most detailed information can not be extracted from Fig.1a. From Fig.1b, only partial detailed information is reflected. From the new transform, say Fig.1c, many detailed insight of the vocalization is captured.

The present acoustic data acquisition system is the same as that used in Ref.[11] which employs a commercial microphone for personal and notebook computers to collect speech or acoustic data. Its specifications are 20-20,000 Hz, 100mw, 32 Ω 105db sound pressure level sensitivity at 1kZ ±2 % and the system uses a 3.5mm stereo jack plug for connection. The data conversion employs the built-in 16 bit recording software of the Micro-Soft Windows XP system.

The first acoustic data was measured on a 6 years old 125 cc KYMCO motorcycle running in a speed of 40 km/hr. The sampling rate is 8000 data per second. The raw data and Fourier sine spectrum are shown in Fig.2a and 2b, respectively. The spectrum shows the engine mode (about 50Hz) and many high harmonics. It is not known why there are many modes with amplitude values scattering around 0.03. Figure 3a through 3c are real part spectrograms of 0.5-200, 200-500, and 500-1000Hz, respectively. The real part plot is employed because it reflects the phase information. From these figures, the frequency shift and amplitude variations of engine mode and harmonics are clearly seen where the amplitude variation is reflected by the dilute and dense level of color. The frequency and amplitude variations of engine mode are not obvious which show the engine condition is not too bad. However, all high harmonics have certain degree of variations because these modes interact with the structure of the motor cycle. Moreover, there are many random vibration modes spread over the whole frequency range. These are modes scattering around amplitude = 0.03. It means that the overall condition of the motor cycle is not good. In fact, the motor cycle had already run 44000 km and had experienced two traffic accidents. This test case shows that the acoustic data reflect the true condition of the sound source.

The second acoustic data was collected at a distance of 10-15 m away from a maneuvered unmanned aerial helicopter (each wing span is about 0.35m) at a height of 3-10m. The raw data and spectrum are shown in Fig.4a and 4b respectively. At the instant about 6.8 seconds, the helicopter was fuel run out of and dropped down to the ground subsequently. There are several dominant modes on the spectrum which are again the fundamental mode of engine and gear box (around 57.1Hz) and harmonics (114, 171, 228, 285, 342, 456, 571, 684, 742, and 1140Hz), the fundamental (around 271-273Hz) and harmonic modes (545, 820, 1090, 1360Hz) of the rotating wings, and the other modes (75, 150, 300, 330, 375, 435, 480, 500, 535, 600, 660, 700, 760, 905Hz). At the low frequency regime, the spectrum shows a complicated mode distribution. Spectrograms of 0-50, 50-100, 0-200, 200-500, 500-1000, 1000-1600 and 1600-3200Hz are shown in Fig.5a through 5f, respectively. From Fig.5a and 5b, there are concentrated information around 0 second and during 2-4 and 8-10 seconds. A careful inspection reveals that they are results of a wind stream rolling around the ground. The authors were not able to hear the wind blowing but it was captured by the microphone and spectrogram as shown. The engine and gear box modes are captured in Fig.5b and 5c. These spectrograms show that the frequency of engine and gear box is slightly drifted in an oscillatory behavior because of aerodynamic loading. In the high harmonics, the degree of frequency variation becomes obvious that may be caused by the nonlinear coupling between gear box, engine and helicopter structure. It is interesting to see that, the following modes have relatively large amplitudes: 114, 228, 456, 684, and 1140Hz. Both the 684 and 1140 Hz modes interact with the rotating wing and wing-tip vortex modes so that has a wideband character. The following modes have a small and may or may not have non-continuous character: 171, 285, 342, 571, and 742 Hz. The fundamental mode of the rotating wings also has a slight frequency variation. Only four harmonics are picked by the spectrogram because the insufficient sampling rate. They are not very clear and show a discontinuous character because the flow field and helicopter structure introduce nonlinear coupling effect. The mechanisms of the other modes are not clear and need further study. The authors guess they are the vibration modes of the helicopter structure modes and twist modes of the rotating wing.

After the fuel run out of instant, all the above mentioned modes reduce their frequencies almost linearly with respect to time. The fundamental engine and gear box modes split into two rows: one linearly decays with respect to time and the other persists for several seconds. The decay mode shows that the rotation speed of the engine slows down. The persisted mode reflects the fact that some components within the gear box still rotate with a constant speed for a while because their angular momentums compensate the effect of engine power reduction.

Those shown in Fig.6a, 6b and 6c are spectrograms of 1600-3200Hz during the period of 0-3, 3-6, and 5.5-9 seconds. This frequency range reflects the wing-tip vortices and the shedding vortices. In the period of 0-2

seconds, there is not wind blowing and the 1800, 2000, 2200, 2430, 2620-2650, and 2900 modes of wing-tip vortices and shedding vortices firmly present. At the period of 2-3 second (as shown in Fig.5a), a wind stream blows through the unmanned helicopter, and the two shedding vortices streets (ridding on the wing-tip vortex lines) are seriously influenced. The more or less regular modes between 2200-2900 Hz now split into several modes as shown. These modes persist until the fuel run out of instant. It seems that the wind stream modifies the flow field structure and vibration behavior of the rotating wings. The recover from the modification takes such a long time reflects that the flow field might become turbulent. After the point, there is no power to support the two wing-tip vortices cores and the shedding vortices stops to be generated. Subsequently, energy of these modes gradually dies out.

The last test case is a sound record taken from Ref.[15]. The F-16 noise is acquired by recording samples from 1/2 inches B&K condensor microphone onto digital audio tape(DAT). The noise was recorded at the co-pilot's seat in a two-seat F-16 fighter, traveling at a speed of 500 knots, and an altitude of 300-600 feet. The sound level during the recording process was 103dB. The sampling rate is 19.98 kHz, the A/D converter uses 16 bit and employs anti-aliasing filter, and the recording time is 235 seconds. The examined case uses a length of 10 seconds. In order to speed up the post processing, the data reduction is made so that only one point is taken from every 10 points.

The spectrograms are shown in Fig.8a through 8d. From Fig.8a, the low frequency vibration modes around 1-20Hz are the vibration of the whole fighter at a low altitude and transonic flight. The 41 and 140 Hz modes are the only two almost persisted wave components. The frequency of these two modes are relatively low and do not have obvious harmonics so that they may be the structure vibration modes of the aircraft structure. There are a series of modes (whose frequency gaps is approximately equal to 40-50 Hz and exist in a non-continuous manner), say 55, 105, 163, 215-220, 270, 325, 378, 430, 485 , 535, 580, 625, 665, 750, 800, 845-850, 885, 935, and 980Hz modes, etc.. All of these modes are believed to be induced by the jet engine's rotor. Besides, there are modes with scattered frequencies around: 70-100, 120-130, 170-190, 220-260, 280-300, 340-360, 400-420, 440-480, 540-560, 590-610, 770-790, 820-830, and 860-870 Hz. These modes may be caused by the interaction between aero-acoustic wave of jet plume and aircraft structure. Since the detailed data of F-16 fight are unavailable, the true mechanisms need a series of careful further studies.

All the above discussions show that a acoustic data string may have a very complicated insight. Nevertheless, they can be captured by the new spectrogram. Now only a fraction of the overall information can be reasonably explained because this is a first study. It is believed that such a technique can be employed to collect practical data in many outdoor environments.

CONCLUSIONS

A new time frequency transform basing on the Fourier sine spectrum is employed to examine three practical acoustic data. The resulting spectrograms show the complicated insight of the data successfully. It is believed that the same technique can be applied to many other engineering problem to study time series data.

ACKNOWLEDGEMENT

This work is supported by the National Science Council of Taiwan, R. O. C. under the grant number NSC-94 -2212-E006-084.

REFERENCES

1. M. Farge, "Wavelet Transforms and Their Applications to Turbulence," *Annu. Rev. Fluid Mech*., vol.24, pp.395-457, 1992.
2. R. Carmona, W. L. Hwang, and B. Torresani, *Practical Time-Frequency Analysis, Gabor and Wavelet Transforms with in Implementation in S*, Academic Press, N. Y. , 1998.
3. *Time-Frequnecy Signal Analysis, Methods and Applic-tions*, ed. by B. Boashash, Longman Cheshire, Australia, 1992.
4. Y. N. Jeng and Y. C. Cheng, "A Simple Strategy to Evaluate the Frequency Spectrum of a Time Series Data with Non-Uniform Intervals," *Trans. Aero. Astro. So., R. O. C*., vol.36, no.3, pp.207-214, 2004.
5. Y. N. Jeng and Y. C. Cheng, "A New Short Time Fourier Transform for a Time Series Data String", to appear in *Trans. Aero. Astro. Soc. R. O. C*., 2006.
6. Y. N. Jeng, C.T. Chen, and Y. C. Cheng, "A New and Effective Tool to Look into Details of a Turbulent Data String," *Proc. 12th National Computational Fluid Dyna-mics Conference*, Kaohsiung Taiwan, paper no. CFD12-2501, Aug. 2005.
7. Y. N. Jeng and Y. C. Cheng, "The New Spectrogram Evaluated by Enhanced Continuous Wavelet and Short Time Fourier Transforms via Windowing Spectrums," *Proc. 18th IPPR conference on Computer Vision, Graphics and Image Processing (CVGIP2005)*, Taipei R. O. C, Aug. 2005, pp.378-383.
8. Y. N. Jeng, C. T. Chen, and Y. C. Cheng, "Studies of Some Detailed Phenomena of a Low Speed Turbulent Flow over a Bluff Body," *Proc. 2005 AASRC/CCAS Joint Conf.*, Kaohsiung, Taiwan, Dec. 2005, paper no. H-47.
9. Y. N. Jeng, C. T. Chen, and Y. C. Cheng, "Some Detailed Information of a Low Speed Turbulent Flow over a Bluff Body Evaluated by New Time-Frequency Analysis," *AIAA* paper no.2006-3340, San Francisco June, 2006.
10. Y. N. Jeng, "Time-Frequency Plot of a Low Speed

Turbulent Flow via a New Time Frequency Transformation," Proc. 16th Combustion Conf., paper no.9001, April, 2006, Taiwan.

11. Y. N. Jeng and Y. C. Cheng, "A Time-Series Data Analyzing System Using a New Time–Frequency Transform", Proc. 2006 International Conference on Innovative Computing, Information and Control, vol. 1, paper no. 0190, pp.525-528, Sept. 30, 2006.
12. Y. N. Jeng, P. G. Huang, and H. Chen, "Filtering and Decomposition of Waveform in Physical Space Using Iterative Moving Least Squares Methods," AIAA paper no.2005-1303, Reno Jan. 2005.
13. Huynh, H. T., "Accurate Monotone Cubic Interpolation," SIAM J. Number. Anal., vol.30, no.1, pp57-100, Feb.1993.
14. Y. N. Jeng, "Modified Hilbert Transform for Non-stationary Data of Finite Range," The 7-th National Computational Fluid Dynamics Conference, P-15 to P-22, Aug. 2000.
15. *F-16 cockpit noise*, Noise-Rom-0 signal.020, NATO: AC243(Panel 3)/RSG-10, Esprit Project no.2589-SAM, produced by Institute for Perception-TNO, The Netherlands Speech Research Unit, RSRE, United Kingdom, Feb 1990.

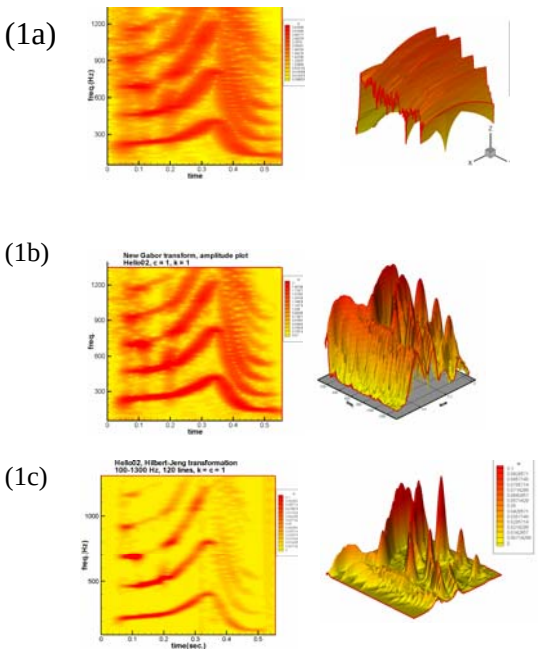

Fig.1 Two and three dimension amplitude plots of the vocalization "hello": (a) the best Gabor transform with a =0.02 sec.; (b) the enhanced Gabor transform where a can be 0.002 to 0.03 sec., $c=1$; and (c) the proposed transform with $c=1$.

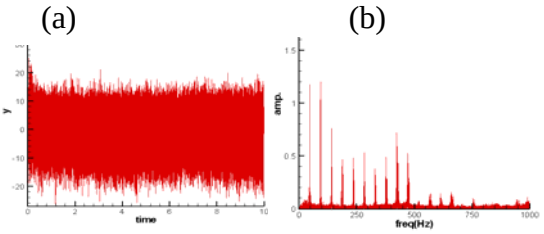

Fig.2 A motorcycle's acoustic data: (a) raw data and (b) Fourier sine spectrum.

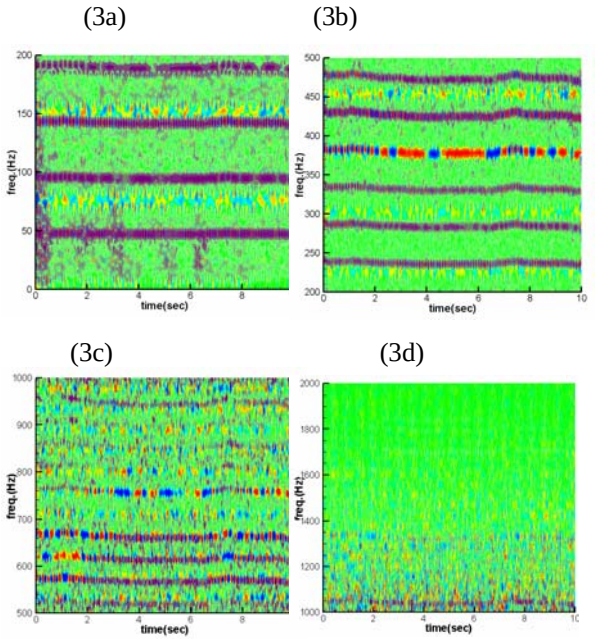

Fig.3 Spectrograms of motorcycle data: (a) 0-200 Hz; (b) 200-500Hz; (c) 500-1000Hz; and (d) 1000-2000Hz.

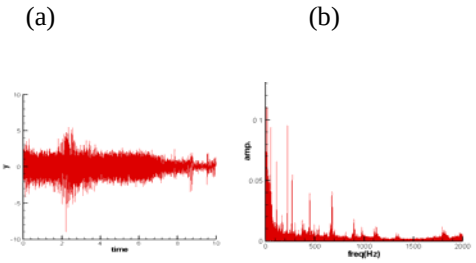

Fig.4 A unmanned helicopter's acoustic data: (a) raw data and (b) Fourier sine spectrum.

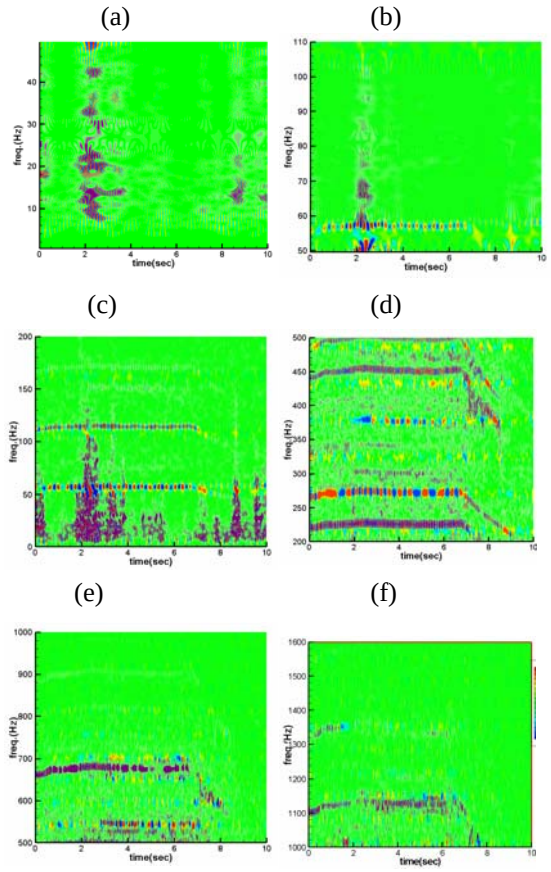

Fig.5 Spectrograms of unmanned helicopter: (a) 0-50Hz; (b) 50-100Hz; (c) 0-200Hz; (d) 200-500Hz; (e) 500-1000Hz; and (f) 1000-1600Hz.

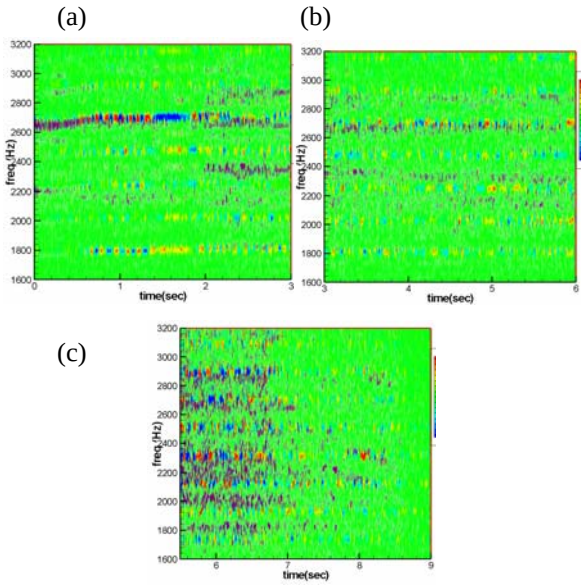

Fig.6 Spectrograms of unmanned helicopter of 1600-3200Hz: (a) 0-3seconds; (b) 3-6 seconds; and (c) 5.5-9 seconds.

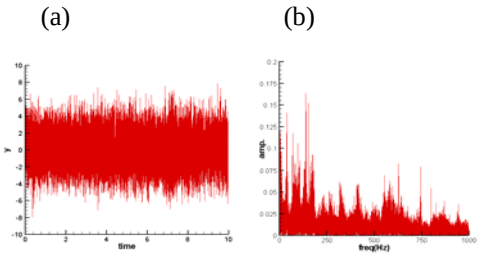

Fig.7 A segment of F-16 acoustic data: (a) raw data and (b) Fourier sine spectrum.

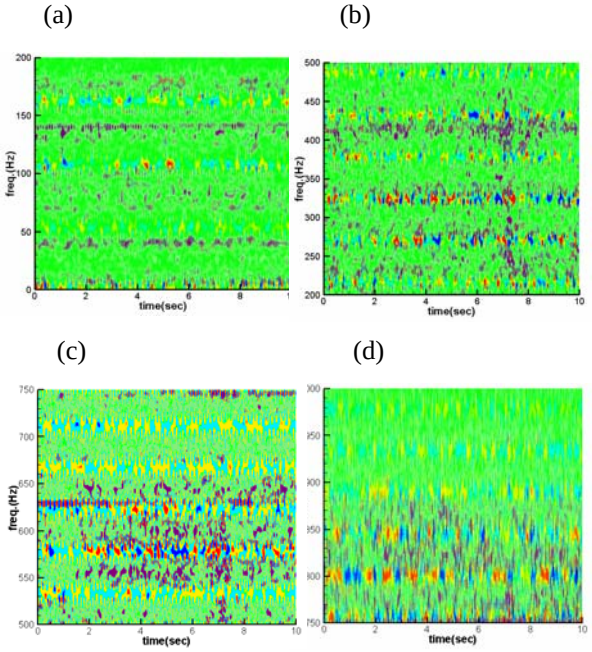

Fig.8 Spectrograms of F-16 Fighter: (a) 0-200Hz; (b) 200-500Hz; (c) 500-750Hz; and (d) 750-1000Hz.